Supplement of The Cryosphere, 17, 5219–5240, 2023
https://doi.org/10.5194/tc-17-5219-2023-supplement

The Cryosphere
Open Access

Supplement of

Multidecadal variability and predictability of Antarctic sea ice in the GFDL SPEAR_LO model

Yushi Morioka et al.

Correspondence to: Yushi Morioka (morioka@jamstec.go.jp)

Supplementary Material

Contents of this file

Fig. S1 to S8

Introduction

This supplementary material provides the initial sea ice states, seasonal cycles of Antarctic sea ice extent (SIE) climatology and decadal sea ice concentration (SIC) variability, the SIC associated with the past two polynya events (1974-1976 and 2016-2017), year-to-year prediction skills of the Antarctic SIC, seasonal dependence of decadal SIC predictability, and normalized predicted SIC anomalies.

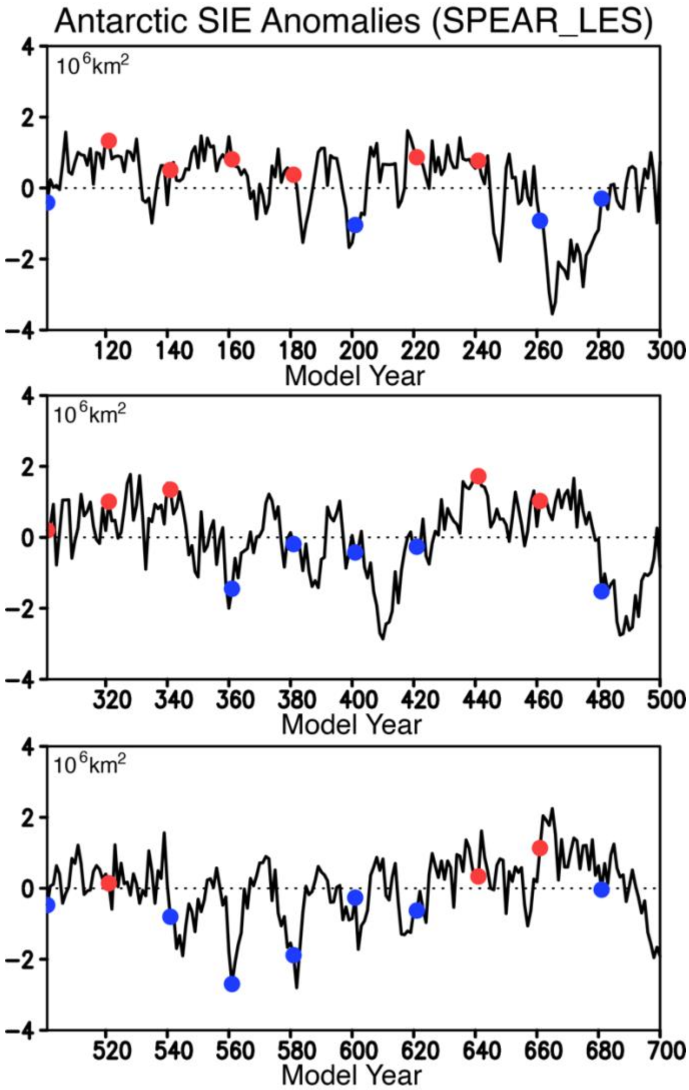

Figure S1 Time series of Antarctic SIE anomalies (in 10^6 km^2) from 101 to 700 years for the SPEAR_LES. Red and blue dots indicates the SPEAR_LO_DCIS start years (101, 121, …, 681 with 20 years interval) with positive and negative SIE anomalies to generate large ensemble members.

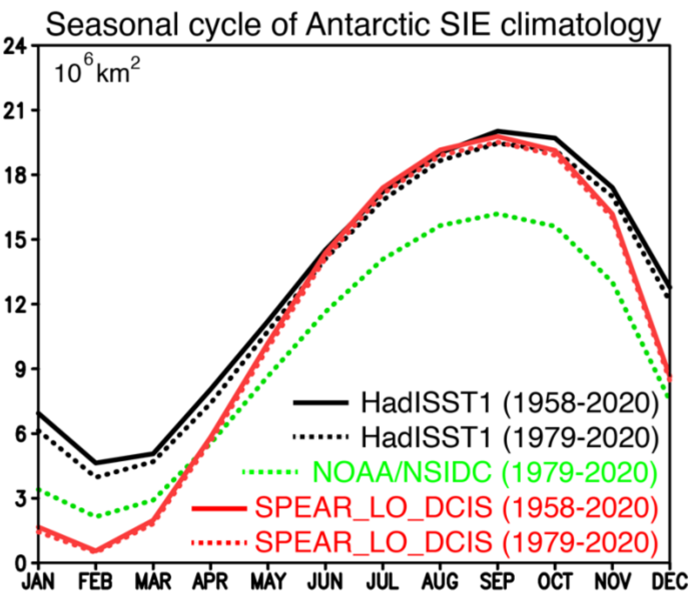

Figure S2 Seasonal cycle of Antarctic sea ice extent (SIE in 10^6 km^2) climatology from the HadISST1 (black), the NOAA/NSIDC (green), and 30 ensemble members average of the SPEAR_LO_DCIS (red). Solid lines indicate the monthly climatology during 1958-2020, while dashed lines represent the climatology during 1979-2020.

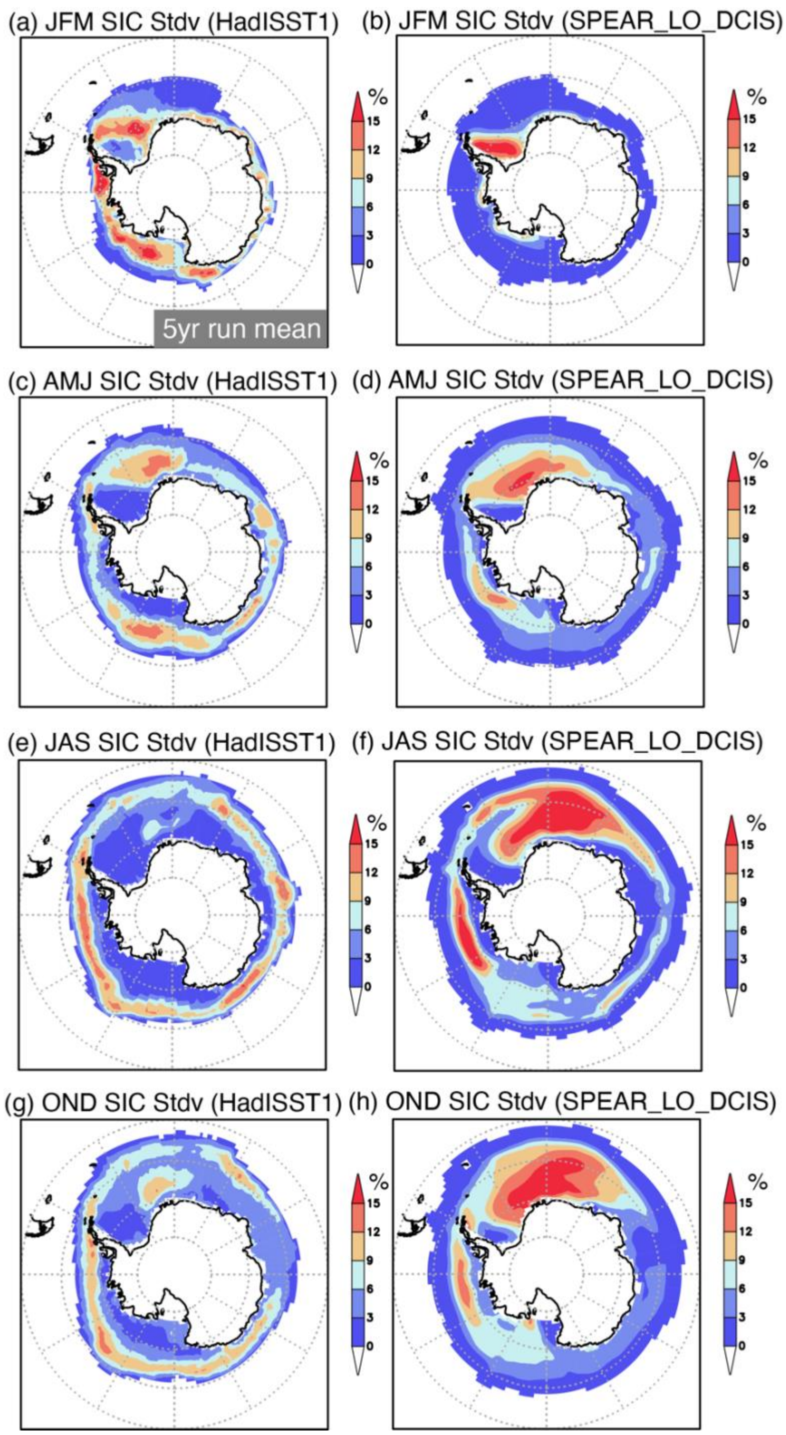

Figure S3 Standard deviation of 5-yr running mean SIC anomalies (in %) during austral summer (January-March; JFM) of 1958-2020 from **(a)** the HadISST1 and **(b)** SPEAR_LO_DCIS. Same as in **(a, b)**, but for **(c, d)** austral autumn (April-June; AMJ), **(e, f)** austral winter (July-September; JAS), and **(g, h)** austral spring (October-December).

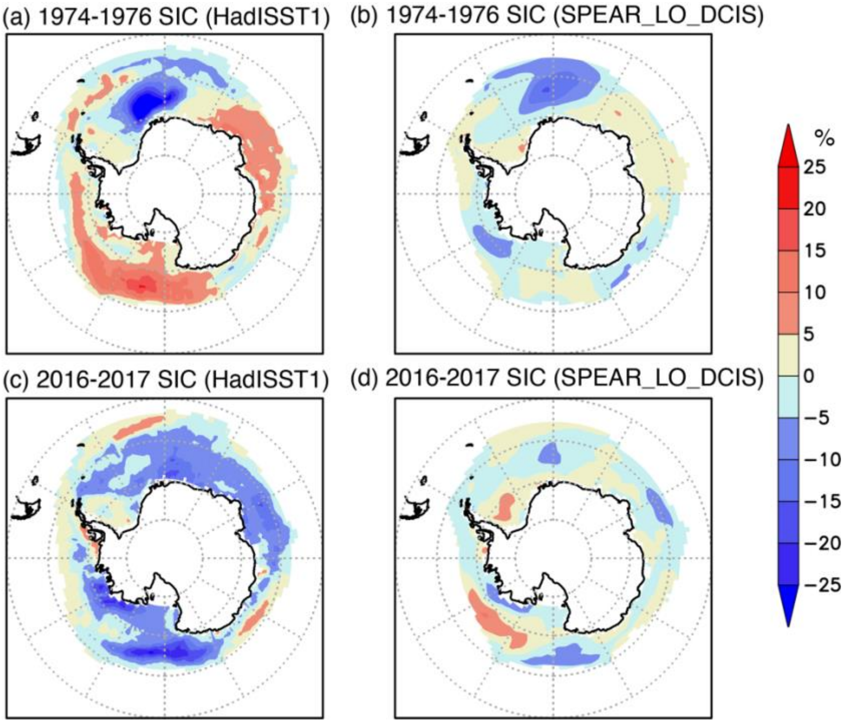

Figure S4 (a) Sea ice concentration (SIC, in %) anomaly averaged over 1974-1976 from the HadISST1. **(b)** Same as in **(a)**, but for the SIC from the SPEAR_LO_DCIS. **(c, d)** Same as in **(a, b)**, but for the SIC anomalies averaged over 2016-2017.

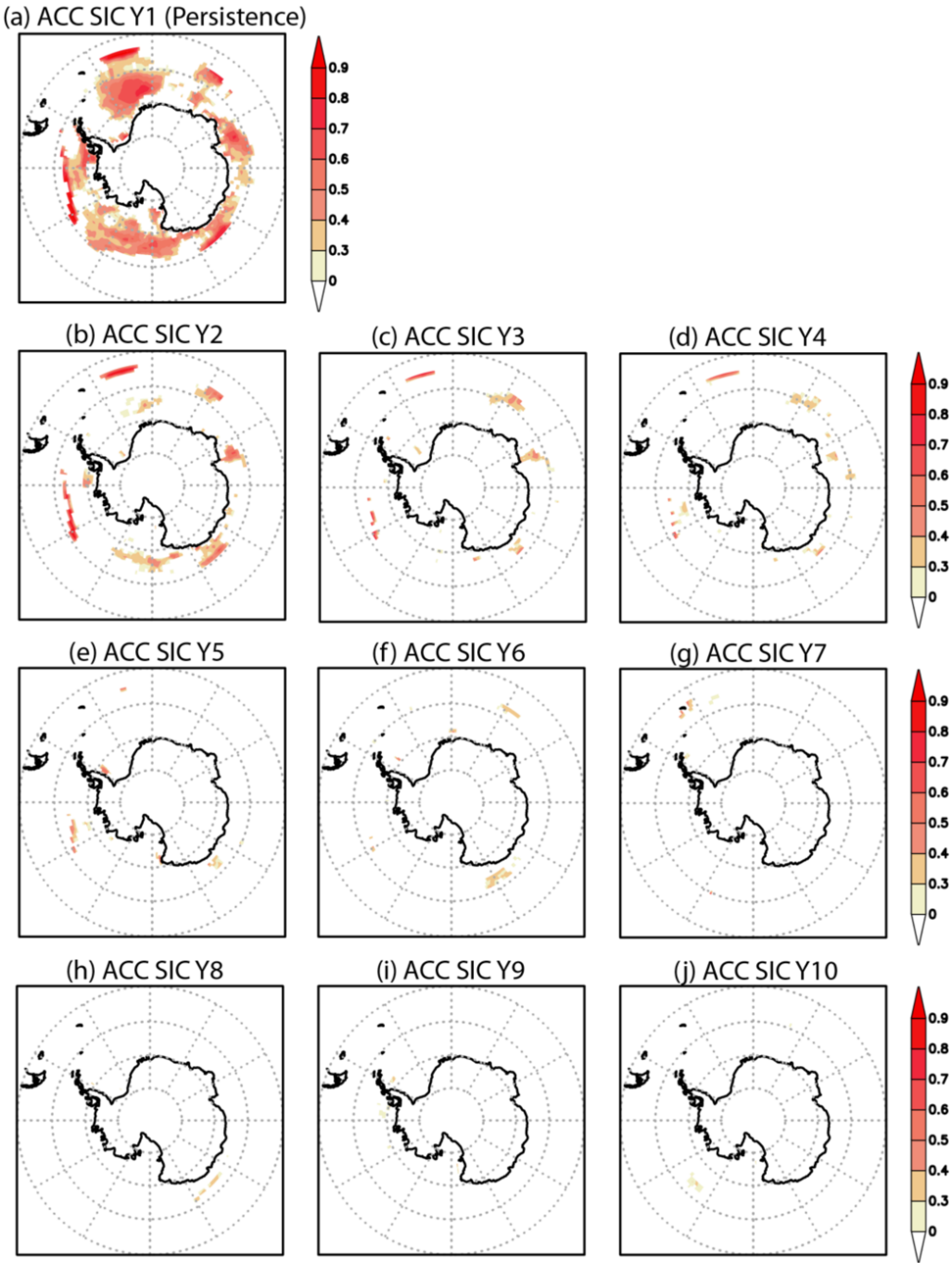

Figure S5 (a) Anomaly correlation (ACC) of the sea ice concentration (SIC) from the persistence prediction based on the HadISST1 during 1961-2020 for the lead time of year 1. Positive ACCs which are statistically significant at 90 % confidence level using Student's *t*-test are colored. **(b-j)** Same as in **(a)**, but for the lead time from year 2 to year 10, respectively.

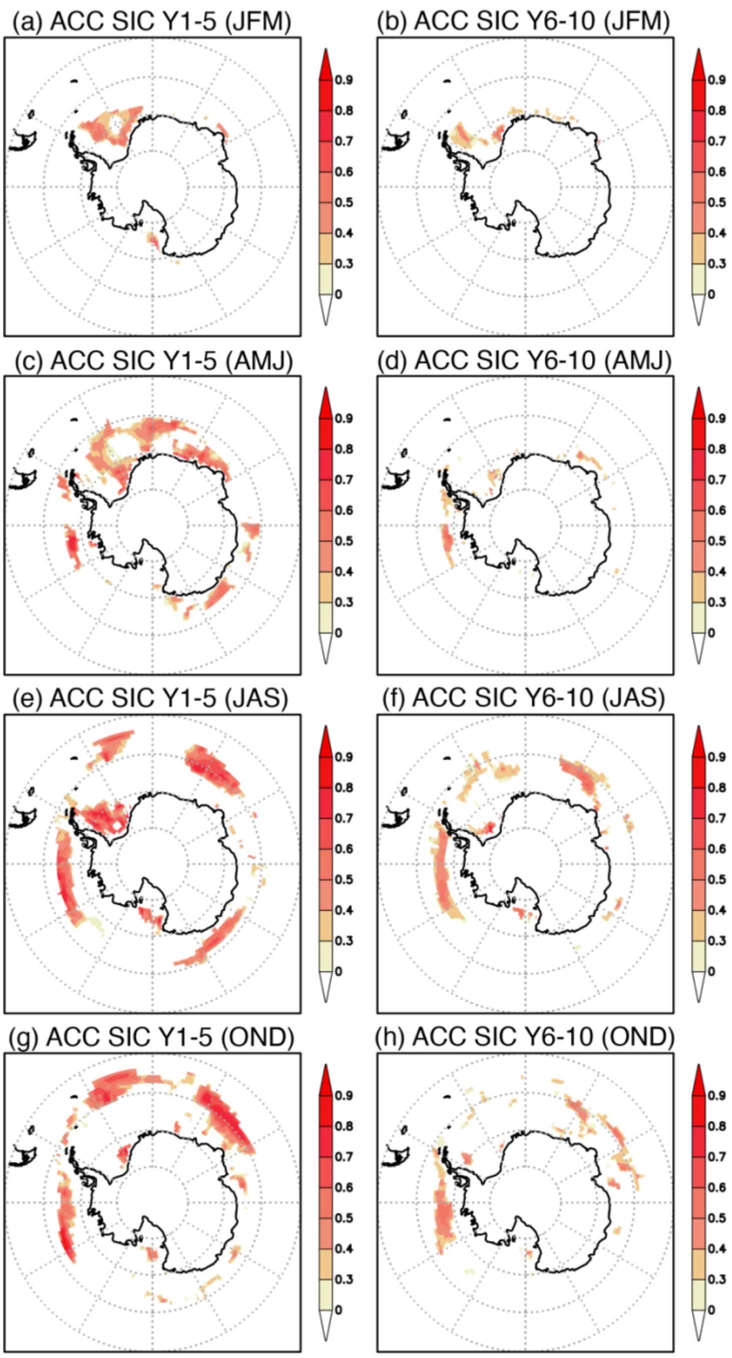

Figure S6 Anomaly correlations between the observed SIC and the predicted SIC from the SPEAR_LO_DRF during austral summer (January-March; JFM) of 1961-2020 for the lead times of **(a)** year 1-5 and **(b)** year 6-10. Positive ACCs which are statistically significant at 90 % confidence level using Student's *t*-test are colored. Same as in **(a, b)**, but for **(c, d)** austral autumn (April-June; AMJ), **(e, f)** winter (July-September; JAS), and **(g, h)** spring (October-December; OND).

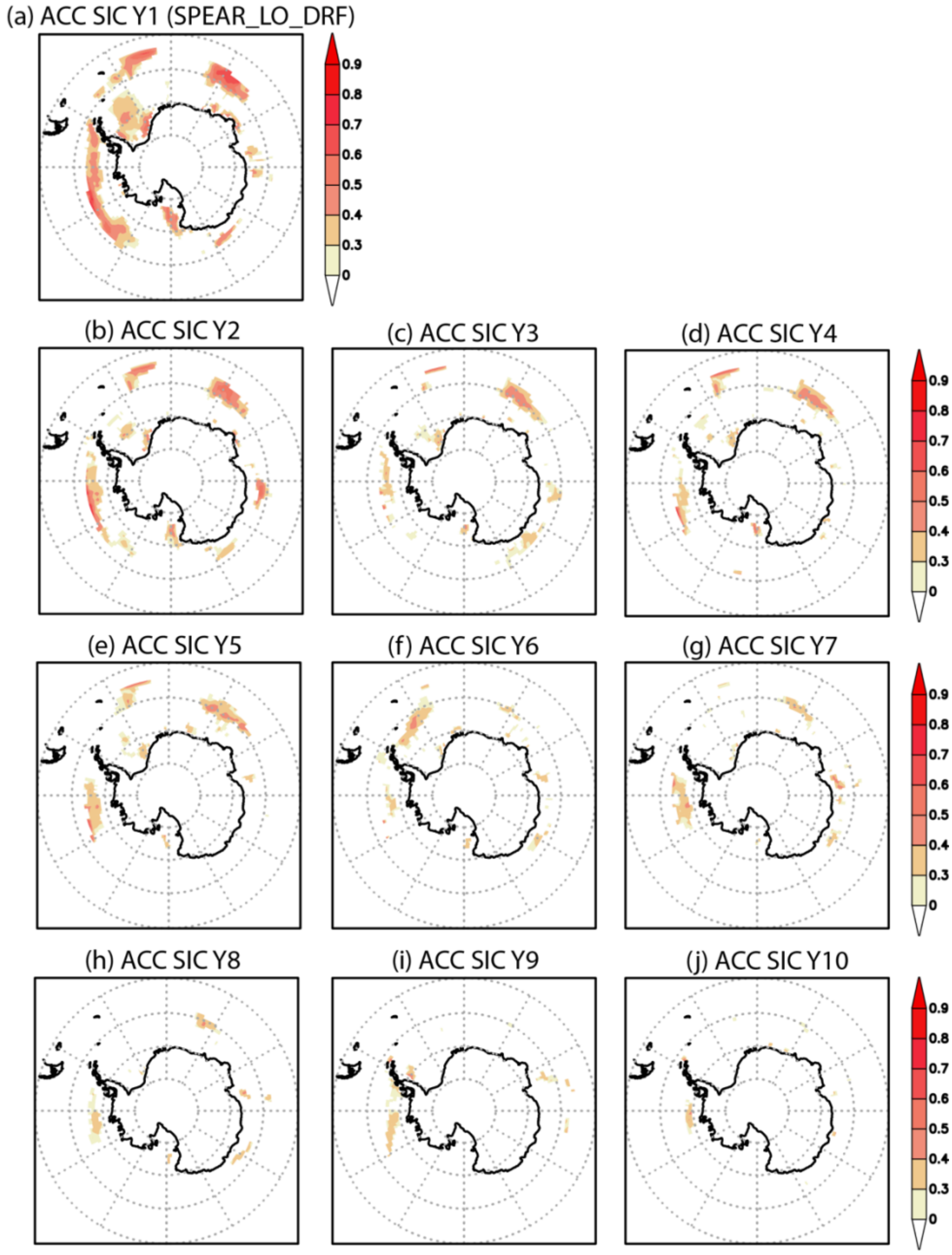

Figure S7 (a) Anomaly correlation (ACC) between the observed SIC and the predicted SIC from the SPEAR_LO_DRF during 1961-2020 for the lead time of year 1. Positive ACCs which are statistically significant at 90 % confidence level using Student's *t*-test are colored. **(b-j)** Same as in **(a)**, but for the lead time from year 2 to year 10, respectively.

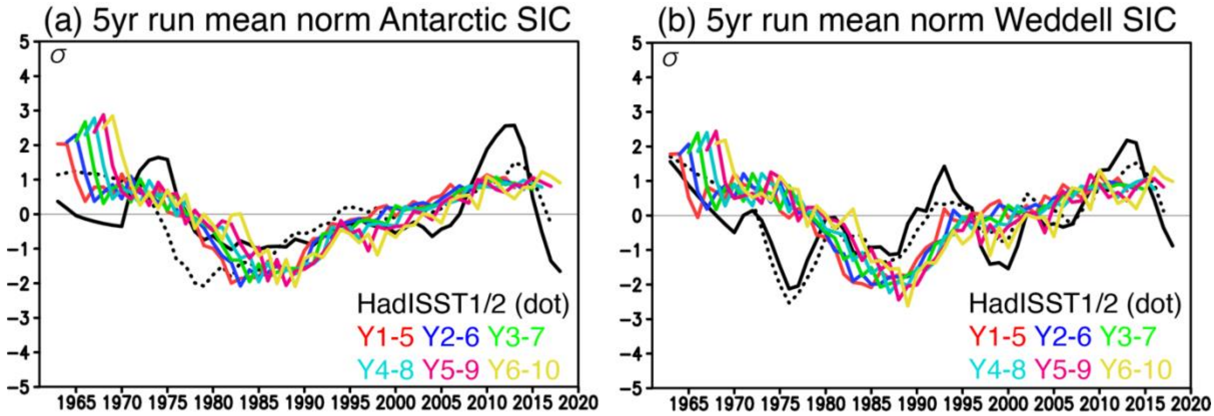

Figure S8 (a) Time series of 5-yr running mean pan-Antarctic SIC (in σ) anomalies normalized by standard deviation (σ) during 1961-2020. Black lines show the observed SIC anomalies from HadISST1 (solid) and HadISST2 (dotted), whereas other colored lines correspond to the ensemble mean normalized SIC anomalies predicted at lead times from 1-5 years to 6-10 years in the SPEAR_LO_DRF. **(b)** Same as in **(a)**, but for the normalized SIC anomalies averaged in the Weddell Sea.